Available online at www.sciencedirect.com
ScienceDirect
Catalysis Today 131 (2008) 197–202
CATALYSIS TODAY
www.elsevier.com/locate/cattod

Photocatalytic activities of $AgSbO_3$ under visible light irradiation

Tetsuya Kako, Naoki Kikugawa, Jinhua Ye *

Photocatalytic Materials Center, National Institute for Materials Science (NIMS), 1-2-1 Sengen, Tsukuba, Ibaraki 305-0047, Japan

Available online 26 November 2007

Abstract

A novel visible light sensitive photocatalyst, $AgSbO_3$ was prepared by a conventional solid-state reaction method. This oxide belonging to a cubic-pyrochlore structure can absorb visible light with wavelength up to about 480 nm. From the band structure calculation, we found that the top of the valence band consists of the hybridized Ag 4d and O 2p orbitals and the bottom of the conduction band mainly consists of the Ag 5s and the Sb 5s orbitals. Photocatalytic activities were evaluated using O_2 evolution from an aqueous silver nitrate solution and decomposition of gaseous 2-propanol under visible light irradiation. We found that $AgSbO_3$ shows a higher O_2 evolution activity than WO_3 and 2-propanol can be mineralized by the $AgSbO_3$ photocatalysis under visible light irradiation.

Keywords: Visible light sensitive photocatalyst; Electronic band structure; O_2 evolution; Decomposition of organics

1. Introduction

Photocatalysis technology has attracted increasing attention because this technology has been widely applied in many products, such as self-cleaning windows and anti-bacterial walls [1,2]. Heterogeneous photocatalysis is a reaction based on the hole and electron pair, which is generated on a semiconductor by illumination with light of energy larger than the band-gap. This photoexcited electron and hole pair provides a redox reaction, which can lead to mineralization of organic chemicals and production of O_2 and/or H_2 from water. Among various photocatalysts, much attention has been paid to anatase TiO_2. However, the use of the TiO_2 photocatalysis is limited to outdoor applications because TiO_2 cannot work under illumination of visible light, which is a main component of the light emitted by an indoor electric lamp.

Therefore, development of the photocatalysts for more efficient utilization of sunlight and the light emitted by an indoor electric lamp has been desirable. Much work has been carried out for development of visible light sensitive photocatalysts [3–12]. Most of the attempts were concentrated on the modification of TiO_2 and Ti-based oxide, such as TiO_2 by doping with a foreign element such as N, C, Cr and V [4–9].

Aside from the doped photocatalysts, some Ag-containing complex oxides, such as $AgNbO_3$ and Ag_3VO_4 have also been reported to be promising visible light sensitive photocatalysts with the band-gap of less than 3.1 eV [11,12]. The tops of the valence band (VB) of the photocatalysts consist of the hybridized Ag 4d and O 2p orbitals. This hybridization is considered to induce the energy at the top of the valance band to a higher energy and make the band-gap narrower. The bottom of the conduction band (CB) consists of the d orbitals of the pentavalent d-block metals, such as the V 3d and the Nb 4d orbitals, which are relatively localized. On the other hand, on a p-block metal containing complex oxide, the bottom of the CB that consists of the less localized s and/or p orbitals is largely dispersed [13]. Because of this large dispersion, p-block metal containing complex oxides were reported to possess high electron mobility and high photocatalytic activity [13,14]. Therefore, Ag- and pentavalent p-block metal (Sb or Bi)-containing complex oxides were considered to be promising visible light sensitive photocatalysts. However, the color of $AgBiO_3$ is black and its band-gap (0.8 eV [15]) is too small for photocatalytic oxidation of the organic compounds [16]. In this study, therefore, $AgSbO_3$ was selected as a candidate of visible light sensitive photocatalysts. Here we investigated the photophysical and photocatalytic properties of $AgSbO_3$ together with calculation of its electronic band structure.

* Corresponding author. Tel.: +81 29 859 2646; fax: +81 29 859 2301.
E-mail address: Jinhua.ye@nims.go.jp (J. Ye).

0920-5861/$ – see front matter
doi:10.1016/j.cattod.2007.10.094

2. Experimental

The $AgSbO_3$ powder was prepared by a conventional solid-state reaction method [17]: stoichiometric amounts of Sb_2O_5 (Kojundo Kagaku Co., Japan) and an excess of 0–3% of Ag_2O (Wako Co., Japan) were mixed well on a mortar and the mixture was calcined at 1173 K for 8 h in an oven. The crystal structure and phase impurity were determined with an X-ray diffractometer (JDX-3500; JEOL Co., Japan) with Cu Kα radiation. The ratio of Ag to Sb was evaluated with an X-ray fluorescence spectrometer (XRF; XRF-1700, Shimadzu Co., Japan). The photophysical property and the specific surface area were evaluated with a UV–vis diffuse reflectance spectrophotometer (UV-2500PC; Shimadzu Co.) and a surface area analyzer (Gemini 2360; Micrometrics Co., USA) by a BET (Brunauer–Emmett–Teller) method at 77 K, respectively.

The photocatalytic activities were evaluated using decomposition of gaseous 2-propanol and evolution of O_2 from an aqueous $AgNO_3$ solution under visible light irradiation. The property of O_2 evolution under visible light irradiation is reported to be important because the photocatalysts capable of O_2 or H_2 evolution are necessary in construction of a Z-scheme system for water splitting [12,18,19].

Decomposition of gaseous 2-propanol into acetone was carried out in a 500-ml glass reactor under visible light irradiation. The powder of 0.4 g of $AgSbO_3$ was spread uniformly over an 8.5-cm^2 area in the center of the base of the reactor. The inside atmosphere was replaced with dry air and then mixed gases comprising dry air and 2-propanol were introduced. By this operation, the concentration of 2-propanol in the reactor became ca. 210 ppm. The reactor was kept in the dark till the adsorption equilibrium state was established. Then visible light (λ: wavelength, 400 nm $< \lambda <$ 530 nm) emitted by a 300-W Xe arc lamp through a water filter and several types of glass filters (Y-44, HA-30 and B390, Hoya Co., Japan) was irradiated. The concentrations of 2-propanol, acetone and CO_2 were measured with a gas chromatograph (GC-14B; Shimadzu) equipped with a flame ionization detector (FID) and a methanizer. The intensity of light irradiated was measured with a spectroradiometer (USR-40D; Ushio Co., Japan) and adjusted to 0.9 mW cm^{-2}.

The experiment of O_2 evolution from an aqueous $AgNO_3$ solution by the $AgSbO_3$ photocatalysis was carried out in a closed gas circulation system [20]. The powder of 0.5 g of $AgSbO_3$ was well dispersed in 270 ml of $AgNO_3$ aq. ($AgNO_3$: 5 mmol) in a glass reactor, prior to visible light irradiation. Then, the reactor was irradiated with visible light ($\lambda > 400$ nm) emitted by a 300-W Xe arc lamp through a UV cutoff filter (L-42, Hoya). The amount of O_2 evolution was measured with a gas chromatograph (GC-8A, Shimadzu) equipped with a thermal conductivity detector (TCD).

The plane-wave-based density functional theory (DFT) calculation of $AgSbO_3$ was performed with the program of Cambridge serial total energy package (CASTEP) [21,22]. The core electrons were replaced by the ultra-soft pseudopotentials.

3. Results and discussion

3.1. Composition

The silver antimonate samples were prepared from initial mixtures of Ag_2O and Sb_2O_5 with nominal Ag/Sb molar ratios ranging from 1.00 to 1.03 (Ag/Sb = 1.00, 1.01 and 1.03). The ratios of Ag to Sb were analyzed with XRF. The analytical Ag/Sb ratios (x) of the silver antimonate (Ag_xSbO_3) samples were estimated to be x = 0.99, 1.00 and 1.02 with the nominal ratios of Ag/Sb = 1.00, 1.01 and 1.03, respectively. The analytical ratios were slightly smaller than the nominal ratios. This may be due to partial volatilization of Ag during calcination at high temperature [11].

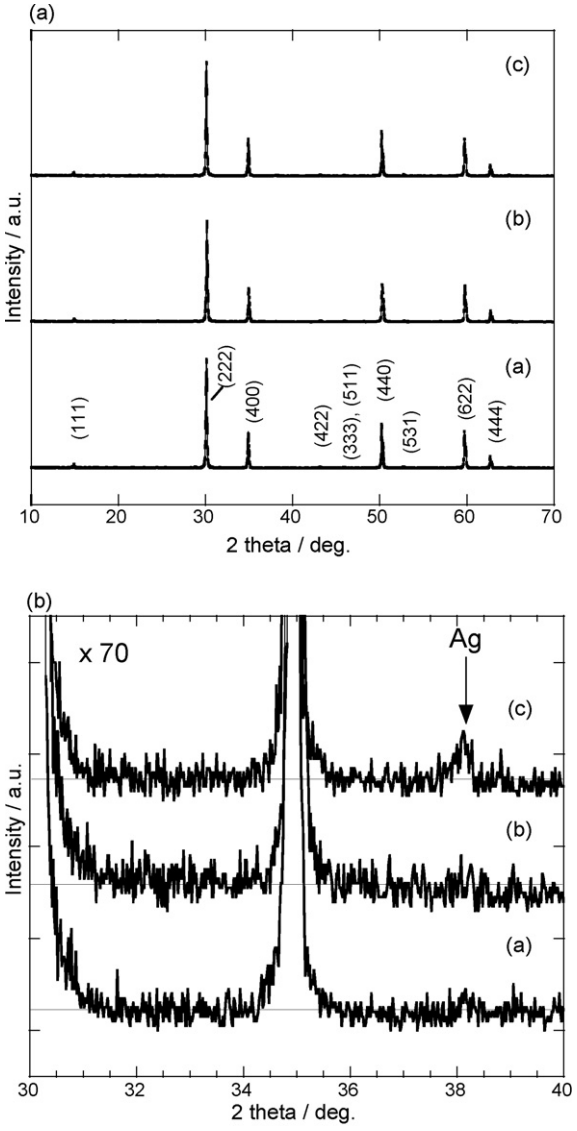

Fig. 1. (a) X-ray diffraction patterns of the prepared samples: (a) $Ag_{0.99}SbO_3$, (b) $Ag_{1.00}SbO_3$ and (c) $Ag_{1.02}SbO_3$. (b) Enlargement of the X-ray diffraction patterns in Fig. 1a: (a) $Ag_{0.99}SbO_3$, (b) $Ag_{1.00}SbO_3$ and (c) $Ag_{1.02}SbO_3$.

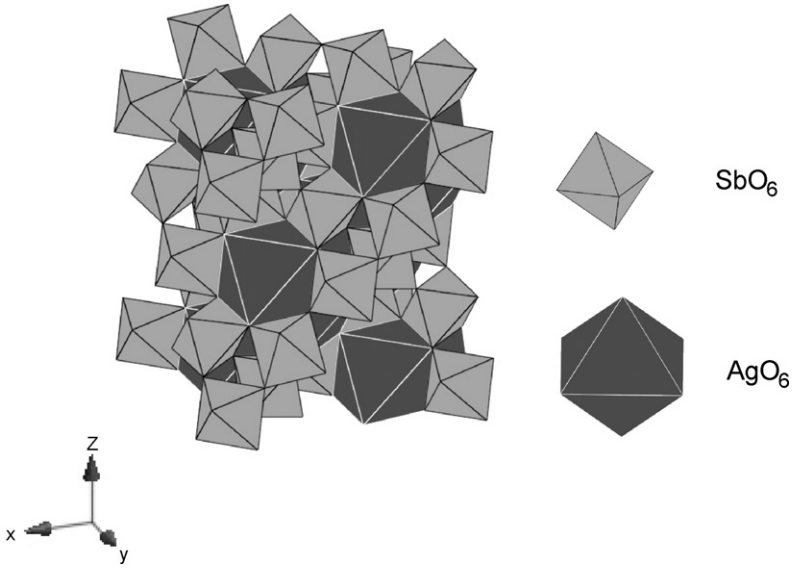

Fig. 2. Illustration of the crystal structure of $AgSbO_3$.

3.2. Crystal structure

The crystal structures and phase impurity of the prepared samples were evaluated with XRD, as shown in Fig. 1. The Ag_xSbO_3 ($x = 0.99$ and 1.00) powders were crystallized in a cubic-pyrochlore structure (space group: *Fd3m*) [23–25]. The XRF and XRD results suggested that the $Ag_{0.99}SbO_3$ powder had a lattice defect at the sites of Ag^+ ions. Also, the $Ag_{1.02}SbO_3$ powder was crystallized into the same cubic-pyrochlore structure, but had a small amount of Ag metal as an impurity (see Fig. 1b). As shown in Fig. 2, the crystal structure of $AgSbO_3$ is constructed by combination of AgO_6 and SbO_6 octahedra. A network of the corner-sharing SbO_6 octahedra forms a parallel hexagonal-prism channel along the (1 1 1) direction.

3.3. Band structure calculation

Photocatalytic activities are dominated by the positions and width of CB and VB. In order to investigate their positions and width, we calculated the electronic band structure of $AgSbO_3$ using the plane-wave-based density functional method [21,22]. Fig. 3 shows the total and the partial density of states (DOS) of bulk $AgSbO_3$. The highest occupied band corresponding to the broad VB was found to consist of the hybridized Ag 4d and O 2p orbitals. This hybridization made the energy at the top of the VB less positive, resulting in a narrower band-gap than that merely consists of O 2p orbitals. We also found that the bottom of the CB in $AgSbO_3$ mainly consists of the Ag 5s and the Sb 5s orbitals (see Fig. 3b). The small contribution of the O 2s and O 2p orbitals to the bottom of the CB can be seen.

3.4. Optical absorption

Fig. 4 shows the optical absorption spectra of the prepared Ag_xSbO_3 samples. The Ag_xSbO_3 ($x = 0.99$ and 1.00) samples whose colors are yellow can absorb up to 480 nm in wavelength

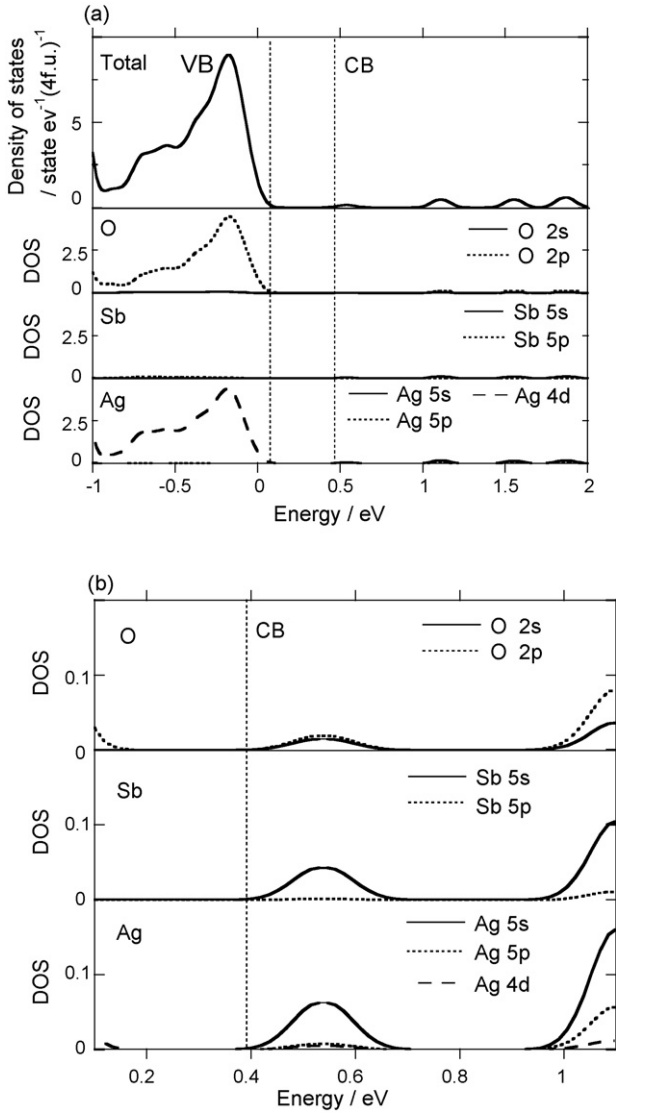

Fig. 3. (a) Total and partial density of states of $AgSbO_3$. (b) Partial density of states of $AgSbO_3$ around the bottom of conduction band.

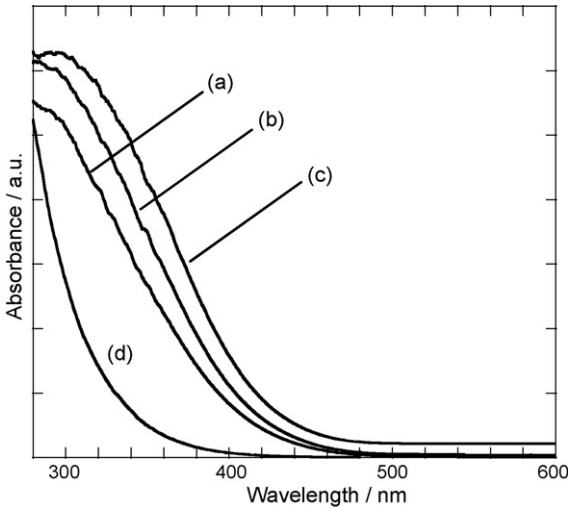

Fig. 4. Optical absorption spectra of the prepared samples and Sb_2O_5: (a) $Ag_{0.99}SbO_3$, (b) $Ag_{1.00}SbO_3$, (c) $Ag_{1.02}SbO_3$ and (d) Sb_2O_5.

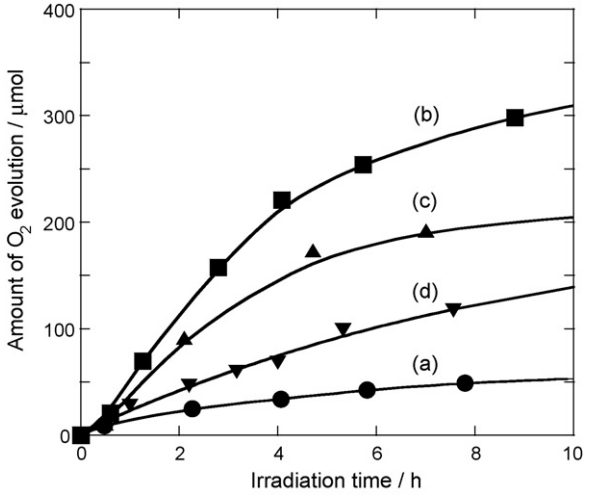

Fig. 6. Evolution of O_2 from an aqueous $AgNO_3$ solution under visible light irradiation in the presence of the prepared samples and WO_3: (a) $Ag_{0.99}SbO_3$, (b) $Ag_{1.00}SbO_3$, (c) $Ag_{1.02}SbO_3$ and (d) WO_3.

of visible light. On the other hand, the spectrum of the gray-green powder $Ag_{1.02}SbO_3$ was characterized by the sharp absorption edge around 480 nm due to the band-gap transition and the long tail over 480 nm which was probably caused by the metallic silver.

As a reference, the absorption spectrum of a starting material Sb_2O_5, whose color is pale lemon yellow, was also measured. As can be expected from the colors, $AgSbO_3$ can absorb a larger amount of visible light than Sb_2O_5. It is apparently shown that the band-gap of $AgSbO_3$ is smaller than that of Sb_2O_5. This band-gap narrowing is caused by hybridization of the Ag 4d and the O 2p orbitals at the top of the VB and by composition of the Ag 5s and the Sb 5s orbitals at the bottom of the CB (Fig. 3).

For qualitative evaluation of the photophysical properties, the optical band-gap energy (E_g) was estimated using a frequently utilized equation:

$$\alpha h\nu = A(h\nu - E_g)^n$$

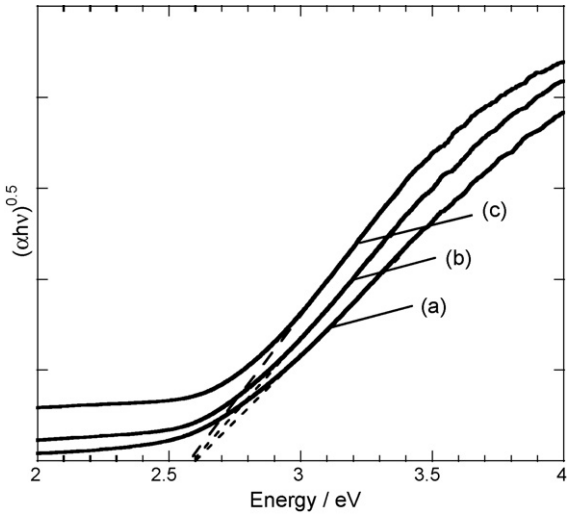

Fig. 5. Estimation of band-gap of the prepared samples: (a) $Ag_{0.99}SbO_3$, (b) $Ag_{1.00}SbO_3$ and (c) $Ag_{1.02}SbO_3$.

Here, α is absorption coefficient near the absorption edge, $h\nu$ is the energy of incident photons, A and n are constant [26,27]. The value of n depends on the transition type. Because $AgSbO_3$ is an indirect transition semiconductor, the value of n is 2 [24]. For estimation of the band-gap, $(\alpha h\nu)^{0.5}$ was plotted against $h\nu$ and then the linear part was extrapolated to zero on an abscissas axis (Fig. 5). From this intercept, the energy gaps of Ag_xSbO_3 ($x = 0.99$, 1.00, and 1.02) were estimated to be 2.6 eV, which were independent of the Ag/Sb ratios.

3.5. Photocatalytic activity

Photocatalytic oxidation activities of the Ag_xSbO_3 powders were evaluated from O_2 evolution as well as decomposition of 2-propanol. Fig. 6 shows O_2 evolution from an aqueous silver nitrate solution in the presence of the prepared Ag_xSbO_3 photocatalysts under visible light irradiation. Upon visible light irradiation, the amount of O_2 evolution increased with an increase in the irradiation time. The initial evolution rates of O_2 over Ag_xSbO_3 ($x = 0.99$, 1.00 and 1.02) were estimated to be about 18, 74 and 50 μmol h^{-1}, respectively. Although having the largest surface area (Table 1), the $Ag_{0.99}SbO_3$ photocatalyst showed the lowest activity among the three compounds. This is possibly because the Ag-defected sites in $Ag_{0.99}SbO_3$ worked as centers of recombination between the photo-generated holes and electrons [28–32]. In photocatalytic decomposition of water over $AgTaO_3$, similar results were also reported [11]. Moreover, the $Ag_{1.02}SbO_3$ photocatalyst partially covered with

Table 1
Surface areas and initial evolution rates of O_2 from an aqueous silver nitrate solution

	Surface area (m^2 g^{-1})	Initial O_2 evolution rate (μmol h^{-1})
$Ag_{0.99}SbO_3$	3.0	18
$Ag_{1.00}SbO_3$	2.5	74
$Ag_{1.02}SbO_3$	2.6	50

metallic Ag showed the lower activity than $Ag_{1.00}SbO_3$. This lower activity may be due to the shielding effect of metallic Ag on the surface of $Ag_{1.02}SbO_3$ [33–35], which led to a decrease in the amount of the active sites for O_2 evolution on the photocatalyst and the amount of visible light absorbed to it.

As a reference, WO_3 was selected because this oxide has been frequently used as a reference photocatalyst for O_2 evolution [11,20]. The activity of O_2 evolution over WO_3 was also evaluated with the same method described above. The rate of O_2 evolution (initial rate, 28 μmol h^{-1}) in the presence of WO_3 (surface area, 5.3 m^2 g^{-1}) under visible light irradiation was lower than that in the presence of $Ag_{1.00}SbO_3$ (74 μmol h^{-1}). The reason why $Ag_{1.00}SbO_3$ showed the higher photocatalytic activity than WO_3 is still unclear because a photocatalytic activity is influenced by many factors, such as band structures, crystallinity, surface areas, adsorption properties, etc. In the present case, however, the following two reasons are most likely. One reason is that the band structure of $AgSbO_3$ at the top of the VB consists of the hybridized Ag 4d and O 2p orbitals that form strong dispersive band, whereas the structure of WO_3 at the top consists of the O 2p orbitals [11,36]. Another reason is that the band structure of $AgSbO_3$ at the bottom of the CB consists of the Ag 5s, Sb 5s, O 2p and O 2s orbitals, leading to a small effective mass of the photo-generated electron. Therefore, the photo-generated electron is considered to migrate more easily to the surface and quickly be consumed by the reaction with $AgNO_3$, resulting in the improvement of charge separation and higher activity of $AgSbO_3$. It is worth describing here that $Ag_{1.00}SbO_3$ may also show the higher activity than $AgNbO_3$ and Ag_3VO_4 because WO_3 was reported and deduced to show the higher O_2 evolution activity than $AgNbO_3$ and Ag_3VO_4 [11,12]. This superiority of the $AgSbO_3$ photocatalytic activity may be due to the differences in the composition of the bottom of CB. The band structures at the bottom of the CB on $AgNbO_3$ and Ag_3VO_4 consist of localized 4d and 3d orbitals, respectively [11,12].

To confirm the stability of $Ag_{1.00}SbO_3$, we compared the XRD patterns before and after experiments, as shown in Fig. 7. Except for the peaks belonging to metallic Ag, no difference between the samples before and after the experiments was observed. To make clear whether the metallic silver is derived from $AgSbO_3$ itself or the Ag^+ in $AgNO_3$ solution, an additional experiment of photocatalytic O_2 evolution from pure water (without $AgNO_3$ sacrificial solution) was carried out. The $AgSbO_3$ sample after 5-h photocatalytic reaction was characterized with XRD. No peaks belonging to the metallic silver were observed. Also, the color of the photocatalyst kept yellow as that before the experiment. No evidence about the formation of metallic silver was obtained in this additional experiment of O_2 evolution from pure water. Therefore, the metallic silver observed in the sample after photocatalytic O_2 evolution from $AgNO_3$ solutions was considered to be derived from reduction of the Ag^+ in $AgNO_3$ solution as reported by many authors [12,37]. These results suggested that $AgSbO_3$ is stable to visible light irradiation under the present experimental conditions.

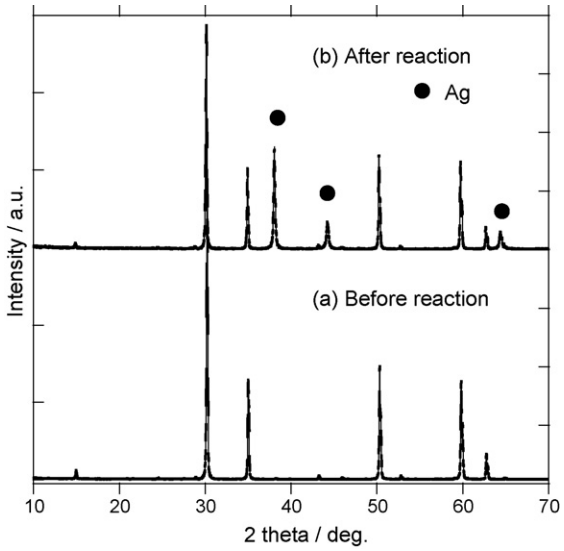

Fig. 7. X-ray diffraction patterns of $Ag_{1.00}SbO_3$ before and after photocatalytic O_2 evolution.

The photocatalytic oxidation properties were also evaluated from decomposition of gaseous organic compounds. Because some visible light sensitive photocatalysts were reported to show relatively high O_2 evolution properties, but low activities for decomposition of gaseous organic compounds [38–40]. These phenomena may be due to the differences in the reaction mechanisms, the necessary oxidizing potentials for the reactions, and so on. As a model of an organic compound, gaseous 2-propanol was selected because this gas is one of the volatile organic compounds (VOCs) and a frequently utilized organic compound for evaluation of a photocatalytic activity. Up to 2-h light irradiation time, no CO_2 and other intermediates except for acetone were detectable in the gas phase. Therefore, the photocatalytic activity was evaluated from the concentration of evolved acetone at the initial stage. Similar evaluations

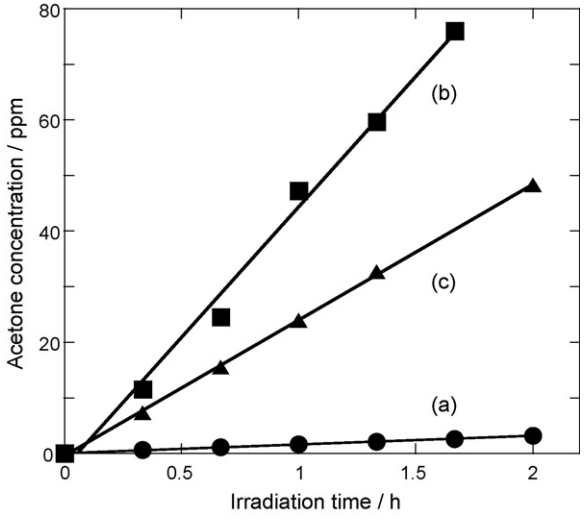

Fig. 8. Generation of acetone from decomposition of 2-propanol under visible light (400 nm < λ < 530 nm) irradiation in the presence of the prepared samples: (a) $Ag_{0.99}SbO_3$, (b) $Ag_{1.00}SbO_3$ and (c) $Ag_{1.02}SbO_3$.

were applied to photocatalytic activities over TiO_2 [41,42]. Fig. 8 shows time dependence of changes in the concentrations of acetone in the presences of the photocatalysts under visible light irradiation. The $Ag_{1.00}SbO_3$ photocatalyst showed the highest activity for decomposition of 2-propanol and $Ag_{0.99}SbO_3$ showed the lowest activity. This order was same as that in O_2 evolution from $AgNO_3$ aq.

Also, we confirmed that upon further visible light irradiation, acetone was oxidized into CO_2 in the presence of the prepared Ag_xSbO_3 photocatalyst. This result suggested that $AgSbO_3$ has an enough strong oxidizing potential to decompose organic compounds into minerals.

We consider that the mechanism of the decomposition of 2-propanol by the $AgSbO_3$ photocatalysis is basically similar to that of TiO_2. However, for clarification of the detail mechanism, further investigation is still required. This subject is now under investigation, and will be reported elsewhere in the near future. In the case of TiO_2 photocatalysis, it was reported that gaseous 2-propanol is selectively oxidized into acetone and acetone is further oxidized into CO_2 via acetaldehyde, acetic acid and formic acid [41,43].

4. Conclusion

The Ag_xSbO_3 photocatalysts with the band-gap of 2.6 eV were prepared by a conventional solid-state reaction method. The band structure by the CASTEP program suggested that the top of the VB and the bottom of the CB mainly consist of the hybridized orbitals of Ag 4d and O 2p and the orbitals of Ag 5s and Sb 5s, respectively. The Ag ion largely contributed to the band-gap narrowing of the antimony-containing oxide, $AgSbO_3$. From the band-gap calculation, $AgSbO_3$ is found to show a strongly dispersive VB. The photocatalytic activity of Ag_xSbO_3 ($x = 0.99$, 1.00 and 1.02) was evaluated from decomposition of 2-propanol and O_2 evolution under visible light irradiation. In both reactions, the order of photocatalytic activities was $Ag_{1.00}SbO_3 > Ag_{1.02}SbO_3 > Ag_{0.99}SbO_3$. The suppression of the photocatalytic activity of the Ag-defected $Ag_{0.99}SbO_3$ photocatalyst is probably attributed from the recombination between the photo-generated holes and electrons. Under strong dispersion, the holes possibly show high migration mobility, which lead to the high activity of this material.

Acknowledgements

This work was partially supported by the Global Environment Research Fund and a Grant-in-Aid for Scientific Research on Priority Areas (417) from the Ministry of Education, Culture, Sports, Science and Technology (MEXT) of the Japanese Government.

Reference

[1] A. Fujishima, K. Hashimoto, T. Watanabe, TiO_2 Photocatalysis Fundamentals and Applications, BKC, Tokyo, 1999.
[2] M.R. Hoffmann, S.T. Martin, W.Y. Choi, D.W. Bahnemann, Chem. Rev. 95 (1995) 69.
[3] K. Maeda, K. Teramura, D.L. Lu, T. Takata, N. Saito, Y. Inoue, K. Domen, Nature 440 (2006) 295.
[4] H. Yamashita, M. Harada, J. Misaka, M. Takeuchi, K. Ikeue, M. Anpo, J. Photochem. Photobiol. A 148 (2002) 257.
[5] R. Asahi, T. Morikawa, T. Ohwaki, K. Aoki, Y. Taga, Science 293 (2001) 269.
[6] T. Ohno, T. Mitsui, M. Matsumura, Chem. Lett. 32 (2003) 364.
[7] H. Irie, Y. Watanabe, K. Hashimoto, Chem. Lett. 32 (2003) 772.
[8] T. Sano, N. Negishi, K. Koike, K. Takeuchi, S. Matsuzawa, J. Mater. Chem. 14 (2004) 380.
[9] Y. Sakatani, H. Ando, K. Okusako, H. Koike, J. Nunoshige, T. Takata, J.N. Kondo, M. Hara, K. Domen, J. Mater. Res. 19 (2004) 2100.
[10] H.G. Kim, D.W. Hwang, J.S. Lee, J. Am. Chem. Soc. 126 (2004) 8912.
[11] H. Kato, H. Kobayashi, A. Kudo, J. Phys. Chem. B 106 (2002) 12441.
[12] R. Konta, H. Kato, H. Kobayashi, A. Kudo, Phys. Chem. Chem. Phys. 5 (2003) 3061.
[13] N. Arai, N. Saito, H. Nishiyama, Y. Inoue, K. Domen, K. Sato, Chem. Lett. 35 (2006) 796.
[14] K. Ikarashi, J. Sato, H. Kobayashi, H. Nishiyama, Y. Inoue, J. Phys. Chem. B 106 (2002) 9048.
[15] H. Mizoguchi, P.M. Woodward, Chem. Mater. 16 (2004) 5233.
[16] Y. Maruyama, H. Irie, K. Hashimoto, J. Phys. Chem. B 110 (2006) 23274.
[17] K.J.D. Mackenzie, F. Golestami-Fard, J. Therm. Anal. 15 (1979) 333.
[18] K. Sayama, R. Yoshida, H. Kusama, K. Okabe, Y. Abe, H. Arakawa, Chem. Phys. Lett. 277 (1997) 387.
[19] K. Sayama, K. Mukasa, R. Abe, Y. Abe, H. Arakawa, J. Photochem. Photobiol. A 148 (2002) 71.
[20] W.F. Yao, J.H. Ye, Catal. Today 116 (2006) 18.
[21] M.D. Segall, P.J.D. Lindan, M.J. Probert, C.J. Pickard, P.J. Hasnip, S.J. Clark, M.C. Payne, J. Phys. Condens. Matter 14 (2002) 2717.
[22] S.J. Clark, M.D. Segall, C.J. Pickard, P.J. Hasnip, M.J. Probert, K. Refson, M.C. Payne, Z. Krystallogr. 220 (2005) 567.
[23] L.G. Berry, B. Post, S. Weissmann, W.F. McClune, Powder Diffraction File, Inorganic sets 1–5, Joint committee on powder diffraction standards, Swarthmore, 1974, p. 246.
[24] H. Hosono, M. Yasukawa, H. Kawazoe, J. Non-Crystal. Solid. 203 (1996) 334.
[25] H. Mizoguchi, H.W. Eng, P.M. Woodward, Inorg. Chem. 43 (2004) 1667.
[26] R. Bacsa, J. Kiwi, T. Ohno, P. Albers, V. Nadtochenko, J. Phys. Chem. B 109 (2005) 5994.
[27] J. Yin, Z. Zou, J. Ye, J. Mater. Res. 17 (2002) 2201.
[28] S. Ikeda, N. Sugiyama, S. Murakami, H. Kominami, Y. Kera, H. Noguchi, K. Uosaki, T. Torimoto, B. Ohtani, Phys. Chem. Chem. Phys. 5 (2003) 778.
[29] B. Ohtani, R.M. Bowman, D.P. Colombo, H. Kominami, H. Noguchi, K. Uosaki, Chem. Lett. 27 (1998) 579.
[30] H. Kato, A. Kudo, J. Phys. Chem. B 106 (2002) 5029.
[31] H. Kato, A. Kudo, J. Phys. Chem. B 105 (2001) 4285.
[32] H. Irie, Y. Watanabe, K. Hashimoto, J. Phys. Chem. B 107 (2003) 5483.
[33] M. Machida, S. Murakami, T. Kijima, S. Matsushima, M. Arai, J. Phys. Chem. B 105 (2001) 3289.
[34] T. Kako, J.H. Ye, Mater. Trans. 46 (2005) 2694.
[35] L. Xiao, J.L. Zhang, Y. Cong, B.Z. Tian, F. Chen, M. Anpo, Catal. Lett. 111 (2006) 207.
[36] M.G. Stachiotti, F. Cora, C.R.A. Catlow, C.O. Rodriguez, Phys. Rev. B 55 (1997) 7508.
[37] H. Kominami, S. Murakami, J. Kato, Y. Kera, B. Ohtani, J. Phys. Chem. B 106 (2002) 10501.
[38] S. Kohtani, S. Makino, A. Kudo, K. Tokumura, Y. Ishigaki, T. Matsunaga, O. Nikaido, K. Hayakawa, R. Nakagaki, Chem. Lett. 31 (2002) 660.
[39] G. Hitoki, T. Takata, J.N. Kondo, M. Hara, H. Kobayashi, K. Domen, Chem. Commun. (2002) 1698.
[40] T. Murase, H. Irie, K. Hashimoto, J. Phys. Chem. B 108 (2004) 15803.
[41] Y. Ohko, K. Hashimoto, A. Fujishima, J. Phys. Chem. A 101 (1997) 8057.
[42] Y. Ohko, A. Fujishima, K. Hashimoto, J. Phys. Chem. B 102 (1998) 1724.
[43] J.M. Coronado, S. Kataoka, I.T. Tejedor, M.A. Anderson, J. Catal. 219 (2003) 219.